Author Manuscript

Author Manuscript

Author Manuscript

Author Manuscript

HHS Public Access

Author manuscript

J Alzheimers Dis. Author manuscript; available in PMC 2017 February 10.

Published in final edited form as:

J Alzheimers Dis. 2016 February 10; 51(2): 571–580. doi:10.3233/JAD-150917.

Increased Electron Paramagnetic Resonance Signal Correlates with Mitochondrial Dysfunction and Oxidative Stress in an Alzheimer's Disease Mouse Brain

Du Fang[a,1], **Zhihua Zhang**[c,a,1], **Hang Li**[c], **Qing Yu**[a,d], **Justin T. Douglas**[b], **Anna Bratasz**[e], **Periannan Kuppusamy**[f], and **Shirley ShiDu Yan**[a,*]

[a]Department of Pharmacology and Toxicology, and Higuchi Bioscience Center, School of Pharmacology, University of Kansas, Lawrence, KS, USA

[b]Nuclear Magnetic Resonance Laboratory, Molecular Structures Group, School of Pharmacy, University of Kansas, Lawrence, KS, USA

[c]School of Life Sciences, Beijing Normal University, Beijing, China

[d]State Key Laboratory of Oral Diseases, West China Hospital of Stomatology, Sichuan University, Cheng Du, China

[e]Small Animal Imaging Core, Ohio State University, Columbus, OH, USA

[f]Department of Radiology, Geisel School of Medicine at Dartmouth College, Hanover, NH, USA

Abstract

Alzheimer's disease (AD) is a progressive neurodegenerative disease characterized clinically by cognitive decline and memory loss. The pathological features are amyloid-β peptide (Aβ) plaques and intracellular neurofibrillary tangles. Many studies have suggested that oxidative damage induced by reactive oxygen species (ROS) is an important mechanism for AD progression. Our recent study demonstrated that oxidative stress could further impair mitochondrial function. In the present study, we adopted a transgenic mouse model of AD (mAPP, overexpressing AβPP/Aβ in neurons) and performed redox measurements using *in vivo* electron paramagnetic resonance (EPR) imaging with methoxycarbamyl-proxyl (MCP) as a redox-sensitive probe for studying oxidative stress in an early stage of pathology in a transgenic AD mouse model. Through assessing oxidative stress, mitochondrial function and cognitive behaviors of mAPP mice at the age of 8–9 months, we found that oxidative stress and mitochondrial dysfunction appeared in the early onset of AD. Increased ROS levels were associated with defects of mitochondrial and cognitive dysfunction. Notably, the *in vivo* EPR method offers a unique way of assessing tissue oxidative stress in living animals under noninvasive conditions, and thus holds a potential for early diagnosis and monitoring the progression of AD.

*Correspondence to: Dr. Shirley ShiDu Yan, Departments of Pharmacology and Toxicology and Higuchi Bioscience Center, School of Pharmacy, University of Kansas, 2099 Constant Ave., Lawrence, KS 66047, USA. Tel.: +1 785 864 3637; s067y548@ku.edu.

[1]These authors contributed equally to this work.

Authors' disclosures available online (http://www.j-alz.com/manuscript-disclosures/15-0917r1).

Author Manuscript Author Manuscript Author Manuscript Author Manuscript

Keywords

Aβ accumulation; cognitive function; mitochondrial dysfunction; oxidative stress

INTRODUCTION

Alzheimer's disease (AD) is a predominant cause of dementia in the elderly population, affecting about 44 million people worldwide in 2015 [1]. AD is pathologically defined by aggregation of amyloid-β (Aβ) peptide that has been derived from pathologically processed amyloid-β protein precursor (AβPP) in extracellular senile plagues and neurofibrillary tangles which consist of hyperphosphorylated tau protein and lead to severe neuronal loss through oxidative stress and neurodegeneration [2, 3]. The mitochondrial dysfunction and increased oxidative stress have been observed in AD-affected brain and mouse model for AD [2, 4, 5]. Oxidative stress leads to an alteration in redox state resulting from an imbalance between the generation and detoxification of reactive oxygen species (ROS), which can be detected in the blood, cerebrospinal fluid, and brain of AD patients [6–9]. ROS plays an important role in many chronic diseases including mitochondrial diseases [10], atherosclerosis [11], diabetes [12], cancer [13], as well as AD [14]. The brain's high energy demand is supplied mostly by OXPHOS, the major producer of free radicals. When the free radical level overwhelms cellular antioxidant defense system, a deleterious condition known as oxidative stress occurs. Oxidative stress and mitochondrial dysfunction can emerge in the course of aging and AD [15, 16]. Considerable data implicate a mechanistically relevant role for ROS in AD. In particular, evidence has suggested that elevated ROS level might increase Aβ production [17]. It is noteworthy that age and lifestyle related AD risk factors, such as hypertension, traumatic brain injury, diabetes mellitus, hyper-cholesterolemia, hyperhomocysteinemia, smoking, high calorie intake, and lack of exercise, are contributors to the increased oxidative stress. There are several reports indicating that oxidative damage precedes the onset of AD pathology [3, 4, 18]. In view of the important role ROS play in health and disease, it is very useful to develop a reliable quantitative noninvasive method for the assessment of oxidative stress in live animals and humans. The present study was aimed at demonstrating electron paramagnetic resonance (EPR) imaging [19, 20] using methoxycarbamyl-proxyl (MCP) as a redox-sensitive probe for visualizing oxidative stress in living subjects and studying oxidative stress and mitochondrial function in the early stage of AD.

MATERIALS AND METHODS

Animals

All the animal studies were approved by the Animal Care and Use Committee of the University of Kansas and Ohio State University in accordance with the National Institutes of Health guidelines for animal care. Transgenic mice (Tg mAPP), both male and female, that overexpress a human mutant form of AβPP bearing both the Swedish (K670N/M671L) and the Indiana (V717F) mutations (APPSwInd, J-20 line, obtained from Jackson Lab) were used in the experiments. The investigators were blinded to the mouse genotype in performing experiments.

Author Manuscript Author Manuscript Author Manuscript Author Manuscript

Electron paramagnetic resonance measurements

In vitro EPR measurements—Intracellular ROS levels were measured using EPR spectroscopy as described in our previous study [21]. Hippocampal slices were incubated with CMH (1-hydroxy-3-methoxycarbonyl-2,2,5,5-tetramethylpyrrolidine; 100 μM) for 30 min, and then washed with cold PBS. The cerebral cortex from Tg mAPP mice and control WT mice were collected and homogenized with 100 μl of PBS for EPR measurement. Samples were loaded into 50 μL BLAUBRAND micropipettes (Sigma), which were sealed with Critoseal (Fisher) and placed in 4 mm EPR tubes (Wilmad Labglass, Vineland, NJ, USA). The EPR spectra were collected, stored, and analyzed with a Bruker EMXplus EPR spectrometer (Billerica, MA, USA) and Bruker software Xenon. The EPR spectrometer was operated at 9.63 GHz and 100 kHz field modulation at room temperature. The spectra were recorded with the following parameters: number of scans, 6; magnetic field center, 344 mT; scan range, 10 mT; microwave power, 2 mW; modulation amplitude, and 0.1 mT; time constant, 0.08 s.

In vivo EPR imaging measurements on live animals—EPR imaging measurements were performed using EPR instrumentation consisting of an L-band EPR spectrometer, three sets of water-cooled gradient coils, and a personal computer-based data acquisition system [19, 20]. EPR spectra were recorded using a custom-built surface resonator. The resonator was capable of sampling a cylindrical volume measuring a diameter of 10 mm and a depth of 5 mm. The open structure of this resonator was ideal for localized measurements on large objects and thus was not limited by the size of the object.

Tg mAPP and littermate control (nonTg) mice at age 8–9 months were anesthetized by administration of ketamine and xylazine. The carotid artery was cannulated with a heparin-filled 30-gauge catheter for infusion of the redox (nitroxide) probe. The hair of the skin on the observation spot (head) was shaved and the animal was placed on a bedplate with a circular slot (20 mm diameter) in such a way that the head was centered at the slot. The animal was secured to the plate with adhesive tape and placed on top of the resonator. An IR lamp was used to maintain normal body temperature, which was measured using a rectal thermistor probe. MCP probe (Alexis) was administered at a dose of 1 μl/g bw at 200 mM concentration *via* carotid artery. EPR measurements were started immediately up on completion of probe infusion. The common carotid artery was occluded during EPR measurement to minimize the effects of blood flow. Projection data were acquired using angular sampling method. The projections were acquired as single scans (1024 points/projection) using constant sweep time. The measured projections were corrected for removal of hyperfine-based artifacts and deconvoluted with the corresponding zero-gradient projection [22]. The deconvoluted projections were then convoluted with a Shepp-Logan filter and subsampled to 128 points for back projection. A single-stage, filtered back projection reconstruction algorithm was used to recover the image.

ROS refer to a number of reactive oxidants including superoxide, hydroxyl, and peroxyl radicals as well as non-radical species including hydrogen peroxide. In most of the cases, such as the study here, superoxide free radicals are the first species generated by the cell/mitochondria while all other species are derived as by-products of superoxide. The

Author Manuscript Author Manuscript Author Manuscript Author Manuscript

superoxide free radical is known to reach with CMH probe, which is EPR silent, and converts it to a nitroxide radical (paramagnetic), which is EPR active and exhibits a characteristic triplet EPR signal. The specificity of CMH for superoxide free radicals has been well established. Thus the appearance of a triplet EPR signal is indicative of superoxide (ROS) and the peak height is a measure of the amount of superoxide accumulation in the tissue.

Aβ measurement

Brain cortical homogenates were incubated in 5-M guanidine HCl and 50-mM Tris HCl (pH 8.0) overnight and then subjected to Aβ concentration detection using human $A\beta_{1-40}$ and $A\beta_{1-42}$ ELISA kits (Invitrogen) following the manufacturer's instructions [18].

Cytochrome c oxidase (CcO) activity assay

Cytochrome *c* oxidase (COX IV) activity was spectrophotometrically determined using Cytochrome *c* Oxidase Assay Kit (Sigma). In brief, cortex of transgenic mAPP mice and non Tg mice were homogenized in the lysis buffer, incubated on ice for 15 min, and centrifuged at 14,000 *g* for 15 min. Suitable volume of supernatants and enzyme solutions were added into 950-μl assay buffer. The reaction was triggered by the addition of 50 μl ferrocytochrome *c* substrate solution (0.22 mM) into the cuvette. The changes in absorbance of cytochrome *c* at 550 nm were recorded immediately using a kinetic program with 5-s delay, 10-s interval, and total 6 readings on an Ultrospect 3100 Pro spectrophotometer.

Measurement of ATP level

ATP levels in cortex were determined using an ATP Bioluminescence Assay Kit (Roche) following the manufacturer's instruction. Mice brain tissues were homogenized in lysis buffer provided in the kit, incubated on ice for 15 min, and centrifuged at 14,000 *g* for 15 min. Subsequent supernatants were measured for the ATP levels using a Luminescence plate reader (Molecular Devices) with an integration time of 10 s.

Behavioral test

The Morris water maze (MWM) test was performed according to the published method [23]. The platform was hidden 0.5–1 cm below the water surface and the white paint was used to better cover the platform. In spatial acquisition session, mice were trained for 6 consecutive days with 4 trials each mouse per day. A trial started with releasing one mouse facing the pool wall and the mouse was allowed to swim freely and search for the escape platform. If the mouse could not reach the platform within 60 s, it was guided to the platform and allowed to stay on for 15 s before the next trial. After all trials, each mouse was dried with paper towels and returned to its own cage. The escape latency was analyzed by the behavior software system (HVS water 2020). On day 7, a probe trial was performed to assess the spatial memory of mice. The platform was removed from the pool and the mice were allowed to swim freely for 60 s. Traces of mice were recorded and data were analyzed by HVS water 2020.

Author Manuscript Author Manuscript Author Manuscript Author Manuscript

Statistical analysis

One-way ANOVA was used for repeated measure analysis, followed by Fisher's protected least significant difference for *post hoc* comparisons. $p < 0.05$ was considered significant. StatView statistics software was used. All data were expressed as the mean ± SEM.

RESULTS

Increased ROS levels in the brain of transgenic mAPP mice

To determine whether oxidative status correlates with AD pathology and mitochondrial dysfunction, transgenic mice overexpressing human Aβ and mutant AβPP (Tg mAPP) were used for our study. Tg mAPP mice have been well-characterized with respect to mitochondrial dysfunction and its associated neuropathological, behavioral, and electrophysiological alterations [5, 24–29]. We used EPR spectroscopy and imaging to measure and map the ROS-mediated tissue oxidative stress in the brain, both *in vitro* and *in vivo*, using a redox-sensitive nitroxyl spin probe MCP. MCP has been used as a blood-brain barrier-permeable nitroxide probe to evaluate redox status [30]. *In vivo* bioreduction of MCP in some tissues, such as tumor tissue, is mostly caused by its reaction with intracellular reductants such GSH and ascorbic acid [20]. However, MCP is also known to react with reactive oxygen radicals, such as superoxide and peroxyl radicals that occur in tissues under oxidative stress; therefore, MCP reduction can be used as a measure of the oxidative stress. The bioreduction of MCP can be measured conveniently in real-time by *in vivo* EPR spectroscopy [30]. The change of EPR signal of MCP injected into animals has been observed as "enhanced signal decay" in various diseases [31–33]. The initial reduction rate of the probe in the brain was determined from a plot of signal intensity versus time, 2–7 min after injection. EPR image of the probe distribution in the brain, *in vivo*, was obtained at approximately 30 min after infusion of the probe. The rate of bioreduction in the Tg mAPP mice was significantly higher than that in the nonTg littermates (Fig. 1), suggesting that the brain tissue of Tg mAPP mice had higher oxidative stress as compared with nonTg mice. To validate the *in vivo* EPR results, we measured ROS in brain tissue homogenates by *in vitro* EPR spectroscopy. The EPR results showed that Tg mAPP mice had significantly enhanced oxidative stress in Aβ-enriched hippocampus and cortex but not in Aβ-spared cerebellum compared to the nonTg littermates at 8–9 months of age in cerebral cortex (Fig. 2). Furthermore, compared to nonTg brain at age of 3 months prior to amyloid deposit in the brain, no significant changes in EPR signal were found in mAPP cortex including hippocampus (date not shown), suggesting that ROS levels correlate to the Aβ accumulation in the brain. The enhanced oxidative stress level measured *in vitro* was similar to the results obtained from the *in vivo* measurements of the redox decay and distribution by EPR spectroscopy and imaging (Fig. 1B). Aβ levels were increased in Tg mAPP cerebral cortex compared with nonTg littermate controls (Fig. 3).

Decline in cytochrome c oxidase activity and ATP levels in mAPP mice

Given that mitochondria are the main sources for ROS and that mitochondrial dysfunction is involved in abnormal accumulation and generation of ROS, we evaluated mitochondrial respiratory function by determining CcO, a key enzyme for complex IV of the mitochondrial respiratory chain, in Tg mAPP mice and nonTg littermate controls. Compared to nonTg

Author Manuscript Author Manuscript Author Manuscript Author Manuscript

mice, mAPP mice showed a significant reduction in CcO activity in the cortex (Fig. 4A). ATP levels, a sign for mitochondrial bioenergy, were significantly decreased in mAPP brain compared with nonTg brain (Fig. 4B). These data suggest the impairment in the mitochondrial respiration and energy metabolism in Aβ-rich brain of AD mice.

Spatial learning and memory impairments in transgenic mAPP mice

In view of the contribution of mitochondrial dysfunction and oxidative stress to the synaptic and cognitive decline, we next examined whether mAPP mice also had impairments in spatial learning and memory. We assessed the spatial learning memory and target searching strategy using MWM. MWM test showed an average latency to locate the hidden platform during each day of training sessions. The transgenic mAPP mice revealed longer latency to locate the hidden platform during the training (Fig. 5A) and reduced the number of times crossing the target (Fig. 5B) and time in the target quadrant (Fig. 5C–D) in the recording period compared to nonTg mice. The mAPP and nonTg mice had similar swimming speed by the visual swimming speed test (Fig. 5E). Thus, the observed difference in spatial learning and memory is a result of defects in cognition but not motility or altered motivation. These data indicate that mAPP mice had significantly impaired spatial learning and memory.

DISCUSSION

AD is an age-related progressive neurodegenerative disease characterized clinically by cognitive decline and memory loss. So far there are no effective treatments to prevent, slow down, or reverse the relentless progression of AD, though significant progresses have been made in understanding its pathogenesis over the past decades. AD can be divided into early versus late onset forms as well as sporadic and autosomal-dominant familial variants. It is necessary to identify persons who are at high risk for developing progressive disease, which are most likely to benefit from early therapeutic intervention. Plenty of data suggest that primary pathological changes including oxidative stress and mitochondria impairment occur prior to Aβ accumulation and tau pathology [34–36]. To verify these assumptions, the key point is whether these changes indeed occur at early AD stages. Using a well-established AD mouse model (mAPP mice) [24, 37] and advanced EPR techniques, we demonstrated that cerebral ROS levels were elevated in mAPP brain at early stage, which negatively correlates to mitochondrial function and learning memory. Oxidative stress is defined by harmful over-production of reactive oxygen/nitrogen species and ROS is mainly derived from the electron transport chain at the mitochondrial inner membrane. Mounting evidences suggest that oxidative stress is an important pathogenic factor in AD and the study for different disease stages showed that 4-hydroxynonenal (a marker of lipid peroxidation) increased significantly in the early stages of AD [4, 38]. Similarly, another marker, F2-isoprostane levels, increased significantly in frontal poles and cerebrospinal fluid from AD patients [39]. In fact, there is evidence showing that oxidative damage is the earliest event in AD progression among all AD hallmarks. Moreover, Aβ can induce oxidative stress and increase production of ROS, both of which impair mitochondrial function. In turn, oxidative stress also promotes Aβ deposition [2, 4, 5, 40], forming a vicious cycle of promoting neurodegeneration. Given the key role of ROS in early onset and progression of AD, developing a highly sensitive and specific probe/method to detect oxidative stress would be

Author Manuscript Author Manuscript Author Manuscript Author Manuscript

critical for studying the initiation of AD and monitoring AD progression. Currently, the most commonly used methods are based on the determination of specific end-products of the damage resulting from oxidative stress including proteins, membrane lipids, and DNA [41, 42]. All these methods are invasive and return an indirect ROS determination. In the present study, we showed *in vitro* and *in vivo* measurements based on EPR spectroscopy and imaging for detecting ROS in the brain of living animals.

The EPR method has become a unique and indispensable tool for the specific detection of reactive oxygen free radicals in biological systems. It has the potential to be used for assessing oxidative stress in humans because of its non-invasiveness. As shown in Figs. 1 and 2, EPR can measure the intracellular ROS in the brain homogenates and in live animals. Given that mitochondria are the major resource of ROS generation and that mitochondrial dysfunction occurs in Aβ-rich mAPP brain, damaged mitochondria from mAPP brain could be a major resource of ROS relevant to amyloid pathology. Indeed, mitochondria-derived superoxide was significantly elevated in mAPP hippocampal and cortical neurons, indicating increased ROS accumulation in Aβ-loaded mitochondria [2, 5]. We have successfully detected increased levels of ROS in Aβ-enriched mAPP brain compared with those from nonTg brain at the age of 8–9 months. Importantly, the ROS levels were not elevated in Aβ- and AD-unaffected cerebellum of the same age of mice, suggesting that oxidative stress occurs in the early onset of AD before severe amyloid accumulation. Mitochondrial dysfunction is one of the early features of the AD-affected brain [3, 40, 43–51]. Impairment of mitochondrial energy metabolism, generation of ROS, and altered activity of the key respiratory enzymes such as CcO are among the earliest detectable defects in AD [3, 44–46, 52–54]. Studies have highlighted the role of mitochondrial Aβ accumulation in the AD pathogenesis. Accumulation of Aβ in mitochondria precedes the extracellular Aβ deposition in the AD brain and increases with age, which is associated with an early onset of loss of synapses, synaptic damage and mitochondrial oxidative damage [18, 27, 28, 48, 51, 55–65]. CcO is a key enzyme involved in the complex IV of the mitochondrial respiratory electron-transport chain. Impairment of CcO disrupts electron flow and may cause mitochondrial respiratory dysfunction [66, 67]. CcO reduction is well-documented at various stages of AD, including early mild cognitive impairment stage [4, 47]. Consistent with our previous results [2], there was a significant reduction in CcO activity in transgenic mAPP mice at the age of 8–9 month, compared to nonTg mice. Similarly, ATP level was reduced significantly in transgenic mAPP mice, suggesting impairment of mitochondrial energy metabolism. Accordingly, oxidative stress and mitochondrial dysfunction intervene in learning and memory as demonstrated by mAPP mice with the impairment of spatial learning and memory. With this highly sensitive and specific EPR imaging protocol using MCP as a redox-sensitive probe for assessing oxidative stress level in the brain of a living animal of AD-type mouse model, the present study demonstrated that elevated levels of ROS in Aβ-rich brain negatively correlate to the extent of mitochondrial and behavioral dysfunction. Except for the minimally invasively surgical intervention to infuse the redox probe into the brain, this *in vivo* EPR method offers a unique way of assessing tissue oxidative stress in living animals under noninvasive conditions. Thus, this *in vivo* approach–the EPR imaging approach–has a great advantage on early diagnostic and monitoring for the progression and treatment of AD by assessing oxidative stress associated with AD pathology.

Author Manuscript Author Manuscript Author Manuscript Author Manuscript

Acknowledgments

This study was supported by grants from the National Institute of Health (R01AG044793, R01NS089116, R37AG037319, R01CA02264). Support for the X-band EPR spectrometer was provided by NSF Chemical Instrumentation Grant # 0946883.

References

1. Van Cauwenberghe C, Van Broeckhoven C, Sleegers K. The genetic landscape of Alzheimer disease: Clinical implications and perspectives. Genet Med. 201510.1038/gim.2015.117
2. Fang D, Wang Y, Zhang Z, Du H, Yan S, Sun Q, Zhong C, Wu L, Vangavaragu JR, Yan S, Hu G, Guo L, Rabinowitz M, Glaser E, Arancio O, Sosunov AA, McKhann GM, Chen JX, Yan SS. Increased neuronal PreP activity reduces Abeta accumulation, attenuates neuroinflammation and improves mitochondrial and synaptic function in Alzheimer disease's mouse model. Hum Mol Genet. 2015; 24:5198–5210. [PubMed: 26123488]
3. Lin MT, Beal MF. Alzheimer's APP mangles mitochondria. Nat Med. 2006; 12:1241–1243. [PubMed: 17088888]
4. Alikhani N, Guo L, Yan S, Du H, Pinho CM, Chen JX, Glaser E, Yan SS. Decreased proteolytic activity of the mitochondrial amyloid-beta degrading enzyme, PreP peptidasome, in Alzheimer's disease brain mitochondria. J Alzheimers Dis. 2011; 27:75–87. [PubMed: 21750375]
5. Du H, Guo L, Fang F, Chen D, Sosunov AA, McKhann GM, Yan Y, Wang C, Zhang H, Molkentin JD, Gunn-Moore FJ, Vonsattel JP, Arancio O, Chen JX, Yan SD. Cyclophilin D deficiency attenuates mitochondrial and neuronal perturbation and ameliorates learning and memory in Alzheimer's disease. Nat Med. 2008; 14:1097–1105. [PubMed: 18806802]
6. Casado A, Encarnacion Lopez-Fernandez M, Concepcion Casado M, de La Torre R. Lipid peroxidation and antioxidant enzyme activities in vascular and Alzheimer dementias. Neurochem Res. 2008; 33:450–458. [PubMed: 17721818]
7. Cristalli DO, Arnal N, Marra FA, de Alaniz MJ, Marra CA. Peripheral markers in neurodegenerative patients and their first-degree relatives. J Neurol Sci. 2012; 314:48–56. [PubMed: 22113180]
8. Sinclair AJ, Bayer AJ, Team M, Johnston J, Warner C, Maxwell SRJ. Altered plasma antioxidant status in subjects with Alzheimer's disease and vascular dementia. Int J Geriat Psychiatry. 1998; 13:840–845.
9. Ihara Y, Hayabara T, Sasaki K, Fujisawa Y, Kawada R, Yamamoto T, Nakashima Y, Yoshimune S, Kawai M, Kibata M, Kuroda S. Free radicals and superoxide dismutase in blood of patients with Alzheimer's disease and vascular dementia. J Neurol Sci. 1997; 153:76–81. [PubMed: 9455982]
10. Enns GM, Kinsman SL, Perlman SL, Spicer KM, Abdenur JE, Cohen BH, Amagata A, Barnes A, Kheifets V, Shrader WD, Thoolen M, Blankenberg F, Miller G. Initial experience in the treatment of inherited mitochondrial disease with EPI-743. Mol Genet Metab. 2012; 105:91–102. [PubMed: 22115768]
11. Drummond GR, Selemidis S, Griendling KK, Sobey CG. Combating oxidative stress in vascular disease: NADPH oxidases as therapeutic targets. Nat Rev Drug Discov. 2011; 10:453–471. [PubMed: 21629295]
12. Karunakaran U, Park KG. A systematic review of oxidative stress and safety of antioxidants in diabetes: Focus on islets and their defense. Diabetes Metab J. 2013; 37:106–112. [PubMed: 23641350]
13. McCarty MF, Barroso-Aranda J, Contreras F. Oxidative stress therapy for solid tumors – A proposal. Med Hypotheses. 2010; 74:1052–1054. [PubMed: 20089364]
14. Jomova K, Vondrakova D, Lawson M, Valko M. Metals, oxidative stress and neurodegenerative disorders. Mol Cell Biochem. 2010; 345:91–104. [PubMed: 20730621]
15. Trifunovic A, Hansson A, Wredenberg A, Rovio AT, Dufour E, Khvorostov I, Spelbrink JN, Wibom R, Jacobs HT, Lars-son NG. Somatic mtDNA mutations cause aging phenotypes without affecting reactive oxygen species production. Proc Natl Acad Sci USA. 2005; 102:17993–17998. [PubMed: 16332961]

Author Manuscript Author Manuscript Author Manuscript Author Manuscript

16. Moreira P, Honda K, Liu Q, Santos M, Oliveira C, Aliev G, Nunomura A, Zhu X, Smith M, Perry G. Oxidative stress: The old enemy in Alzheimer's disease Pathophysiology. Curr Alzheimer Res. 2005; 2:403–408. [PubMed: 16248845]
17. Tong Y, Zhou W, Fung V, Christensen MA, Qing H, Sun X, Song W. Oxidative stress potentiates BACE1 gene expression and Aβ generation. J Neural Transm. 2005; 112:455–469. [PubMed: 15614428]
18. Du H, Guo L, Yan S, Sosunov AA, McKhann GM, Yan SS. Early deficits in synaptic mitochondria in an Alzheimer's disease mouse model. Proc Natl Acad Sci U S A. 2010; 107:18670–18675. [PubMed: 20937894]
19. Kuppusamy P, Afeworki M, Shankar RA, Coffin D, Krishna MC, Hahn SM, Mitchell JB, Zweier JL. *In vivo* electron paramagnetic resonance imaging of tumor heterogeneity and oxygenation in a murine model. Cancer Res. 1998; 58:1562–1568. [PubMed: 9537265]
20. Kuppusamy P, Li H, Ilangovan G, Cardounel AJ, Zweier JL, Yamada K, Krishna MC, Mitchell JB. Noninvasive imaging of tumor redox status and its modification by tissue glutathione levels. Cancer Res. 2002; 62:307–312. [PubMed: 11782393]
21. Gan X, Wu L, Huang S, Zhong C, Shi H, Li G, Yu H, Howard Swerdlow R, Xi Chen J, Yan SS. Oxidative stress-mediated activation of extracellular signal-regulated kinase contributes to mild cognitive impairment-related mitochondrial dysfunction. Free Radic Biol Med. 2014; 75:230–240. [PubMed: 25064321]
22. Kuppusamy P, Zweier JL. A forward-subtraction procedure for removing hyperfine artifacts in electron paramagnetic resonance imaging. Magn Reson Med. 1996; 35:316–322. [PubMed: 8699942]
23. Vorhees CV, Williams MT. Morris water maze: Procedures for assessing spatial and related forms of learning and memory. Nat Protoc. 2006; 1:848–858. [PubMed: 17406317]
24. Mucke L, Masliah E, Yu GQ, Mallory M, Rockenstein EM, Tatsuno G, Hu K, Kholodenko D, Johnson-Wood K, McConlogue L. High-level neuronal expression of abeta 1–42 in wild-type human amyloid protein precursor transgenic mice: Synaptotoxicity without plaque formation. J Neurosci. 2000; 20:4050–4058. [PubMed: 10818140]
25. Caspersen C, Wang N, Yao J, Sosunov A, Chen X, Lustbader JW, Xu HW, Stern D, McKhann G, Yan SD. Mitochondrial Abeta: A potential focal point for neuronal metabolic dysfunction in Alzheimer's disease. FASEB J. 2005; 19:2040–2041. [PubMed: 16210396]
26. Arancio O, Zhang HP, Chen X, Lin C, Trinchese F, Puzzo D, Liu S, Hegde A, Yan SF, Stern A, Luddy JS, Lue LF, Walker DG, Roher A, Buttini M, Mucke L, Li W, Schmidt AM, Kindy M, Hyslop PA, Stern DM, Du Yan SS. RAGE potentiates Abeta-induced perturbation of neuronal function in transgenic mice. EMBO J. 2004; 23:4096–4105. [PubMed: 15457210]
27. Lustbader JW, Cirilli M, Lin C, Xu HW, Takuma K, Wang N, Caspersen C, Chen X, Pollak S, Chaney M, Trinchese F, Liu S, Gunn-Moore F, Lue LF, Walker DG, Kuppusamy P, Zewier ZL, Arancio O, Stern D, Yan SS, Wu H. ABAD directly links Abeta to mitochondrial toxicity in Alzheimer's disease. Science. 2004; 304:448–452. [PubMed: 15087549]
28. Takuma K, Yao J, Huang J, Xu H, Chen X, Luddy J, Trillat AC, Stern DM, Arancio O, Yan SS. ABAD enhances Abeta-induced cell stress via mitochondrial dysfunction. FASEB J. 2005; 19:597–598. [PubMed: 15665036]
29. Du H, Guo L, Zhang W, Rydzewska M, Yan S. Cyclophilin D deficiency improves mitochondrial function and learning/memory in aging Alzheimer disease mouse model. Neurobiol Aging. 2011; 32:398–406. [PubMed: 19362755]
30. Emoto MC, Sato-Akaba H, Hirata H, Fujii HG. Dynamic changes in the distribution and time course of blood-brain barrier-permeative nitroxides in the mouse head with EPR imaging: Visualization of blood flow in a mouse model of ischemia. Free Radic Biol Med. 2014; 74:222–228. [PubMed: 25014567]
31. Article J, Shingo M, Ichiro K, Toyoshi I, Hajime N, Hideo U. Confirmation of superoxide generation via xanthine oxidase in streptozotocin-induced diabetic mice. Free Radic Res. 2003; 37:767–772. [PubMed: 12911273]

Author Manuscript Author Manuscript Author Manuscript Author Manuscript

32. Phumala N, Ide T, Utsumi H. Noninvasive evaluation of *in vivo* free radical reactions catalyzed by iron using *in vivo* ESR spectroscopy. Free Radic Biol Med. 1999; 26:1209–1217. [PubMed: 10381192]
33. Yamada KI, Kuppusamy P, English S, Yoo J, Irie A, Subramanian S, Mitchell JB, Krishna MC. Feasibility and assessment of non-invasive *in vivo* redox status using electron paramagnetic resonance imaging. Acta Radiol. 2002; 43:433–440. [PubMed: 12225490]
34. Krstic D, Knuesel I. Deciphering the mechanism underlying late-onset Alzheimer disease. Nat Rev Neurol. 2013; 9:25–34. [PubMed: 23183882]
35. Castellani RJ, Perry G. The complexities of the pathology-pathogenesis relationship in Alzheimer disease. Biochem Pharmacol. 2014; 88:671–676. [PubMed: 24447936]
36. Small SA, Duff K. Linking Abeta and tau in late-onset Alzheimer's disease: A dual pathway hypothesis. Neuron. 2008; 60:534–542. [PubMed: 19038212]
37. Shineman DW, Basi GS, Bizon JL, Colton CA, Greenberg BD, Hollister BA, Lincecum J, Leblanc GG, Lee LB, Luo F, Morgan D, Morse I, Refolo LM, Riddell DR, Scearce-Levie K, Sweeney P, Yrjanheikki J, Fillit HM. Accelerating drug discovery for Alzheimer's disease: Best practices for preclinical animal studies. Alzheimers Res Ther. 2011; 3:28. [PubMed: 21943025]
38. Bradley MA, Xiong-Fister S, Markesbery WR, Lovell MA. Elevated 4-hydroxyhexenal in Alzheimer's disease (AD) progression. Neurobiol Aging. 2012; 33:1034–1044. [PubMed: 20965613]
39. Praticò D, Lee VM-Y, Trojanowski JQ, Rokach J, Fitzgerald GA. Increased F2-isoprostanes in Alzheimer's disease – evidence for enhanced lipid peroxidation *in vivo*. FASEB J. 1998; 12:1777–1783. [PubMed: 9837868]
40. Cardoso SM, Santana I, Swerdlow RH, Oliveira CR. Mitochondria dysfunction of Alzheimer's disease cybrids enhances Abeta toxicity. J Neurochem. 2004; 89:1417–1426. [PubMed: 15189344]
41. Holley AE, Cheeseman KH. Measuring free radical reactions *in vivo*. Br Med Bull. 1993; 49:494–505. [PubMed: 8221018]
42. Kohen R, Nyska A. Oxidation of biological systems: Oxidative stress phenomena, antioxidants, redox reactions, and methods for their quantification. Toxicol Pathol. 2002; 30:620–650. [PubMed: 12512863]
43. Reddy PH. Mitochondrial medicine for aging and neurodegenerative diseases. Neuromolecular Med. 2008; 10:291–315. [PubMed: 18566920]
44. Maurer I, Zierz S, Moller HJ. A selective defect of cytochrome c oxidase is present in brain of Alzheimer disease patients. Neurobiol Aging. 2000; 21:455–462. [PubMed: 10858595]
45. Blass JP. The mitochondrial spiral. An adequate cause of dementia in the Alzheimer's syndrome. Ann N Y Acad Sci. 2000; 924:170–183. [PubMed: 11193795]
46. Sheehan JP, Swerdlow RH, Miller SW, Davis RE, Parks JK, Parker WD, Tuttle JB. Calcium homeostasis and reactive oxygen species production in cells transformed by mitochondria from individuals with sporadic Alzheimer's disease. J Neurosci. 1997; 17:4612–4622. [PubMed: 9169522]
47. Valla J, Schneider L, Niedzielko T, Coon KD, Caselli R, Sabbagh MN, Ahern GL, Baxter L, Alexander G, Walker DG, Reiman EM. Impaired platelet mitochondrial activity in Alzheimer's disease and mild cognitive impairment. Mitochondrion. 2006; 6:323–330. [PubMed: 17123871]
48. Reddy PH, Beal MF. Amyloid beta, mitochondrial dysfunction and synaptic damage: Implications for cognitive decline in aging and Alzheimer's disease. Trends Mol Med. 2008; 14:45–53. [PubMed: 18218341]
49. Leuner K, Hauptmann S, Abdel-Kader R, Scherping I, Keil U, Strosznajder JB, Eckert A, Muller WE. Mitochondrial dysfunction: The first domino in brain aging and Alzheimer's disease? Antioxid Redox Signal. 2007; 9:1659–1675. [PubMed: 17867931]
50. Hauptmann S, Scherping I, Drose S, Brandt U, Schulz KL, Jendrach M, Leuner K, Eckert A, Muller WE. Mitochondrial dysfunction: An early event in Alzheimer pathology accumulates with age in AD transgenic mice. Neurobiol Aging. 2009; 30:1574–1586. [PubMed: 18295378]
51. Yao J, Irwin RW, Zhao L, Nilsen J, Hamilton RT, Brinton RD. Mitochondrial bioenergetic deficit precedes Alzheimer's pathology in female mouse model of Alzheimer's disease. Proc Natl Acad Sci USA. 2009; 106:14670–14675. [PubMed: 19667196]

Author Manuscript Author Manuscript Author Manuscript Author Manuscript

52. Blass JP. Cerebrometabolic abnormalities in Alzheimer's disease. Neurol Res. 2003; 25:556–566. [PubMed: 14503009]
53. Swerdlow RH, Khan SM. A "mitochondrial cascade hypothesis" for sporadic Alzheimer's disease. Med Hypotheses. 2004; 63:8–20. [PubMed: 15193340]
54. Swerdlow RH, Khan SM. The Alzheimer's disease mitochondrial cascade hypothesis: An update. Exp Neurol. 2009; 218:308–315. [PubMed: 19416677]
55. Chui DH, Dobo E, Makifuchi T, Akiyama H, Kawakatsu S, Petit A, Checler F, Araki W, Takahashi K, Tabira T. Apoptotic neurons in Alzheimer's disease frequently show intracellular Abeta42 labeling. J Alzheimers Dis. 2001; 3:231–239. [PubMed: 12214064]
56. Chui DH, Tanahashi H, Ozawa K, Ikeda S, Checler F, Ueda O, Suzuki H, Araki W, Inoue H, Shirotani K, Takahashi K, Gallyas F, Tabira T. Transgenic mice with Alzheimer presenilin 1 mutations show accelerated neurodegeneration without amyloid plaque formation. Nat Med. 1999; 5:560–564. [PubMed: 10229234]
57. Oddo S, Caccamo A, Shepherd JD, Murphy MP, Golde TE, Kayed R, Metherate R, Mattson MP, Akbari Y, LaFerla FM. Triple-transgenic model of Alzheimer's disease with plaques and tangles: Intracellular Abeta and synaptic dysfunction. Neuron. 2003; 39:409–421. [PubMed: 12895417]
58. Hsia AY, Masliah E, McConlogue L, Yu GQ, Tatsuno G, Hu K, Kholodenko D, Malenka RC, Nicoll RA, Mucke L. Plaque-independent disruption of neural circuits in Alzheimer's disease mouse models. Proc Natl Acad Sci U S A. 1999; 96:3228–3233. [PubMed: 10077666]
59. Li QX, Maynard C, Cappai R, McLean CA, Cherny RA, Lynch T, Culvenor JG, Trevaskis J, Tanner JE, Bailey KA, Czech C, Bush AI, Beyreuther K, Masters CL. Intra-cellular accumulation of detergent-soluble amyloidogenic A beta fragment of Alzheimer's disease precursor protein in the hippocampus of aged transgenic mice. J Neurochem. 1999; 72:2479–2487. [PubMed: 10349858]
60. Takahashi RH, Milner TA, Li F, Nam EE, Edgar MA, Yamaguchi H, Beal MF, Xu H, Greengard P, Gouras GK. Intraneuronal Alzheimer abeta42 accumulates in multivesicular bodies and is associated with synaptic pathology. Am J Pathol. 2002; 161:1869–1879. [PubMed: 12414533]
61. Reddy PH, McWeeney S, Park BS, Manczak M, Gutala RV, Partovi D, Jung Y, Yau V, Searles R, Mori M, Quinn J. Gene expression profiles of transcripts in amyloid precursor protein transgenic mice: Up-regulation of mitochondrial metabolism and apoptotic genes is an early cellular change in Alzheimer's disease. Hum Mol Genet. 2004; 13:1225–1240. [PubMed: 15115763]
62. Reddy PH, Mani G, Park BS, Jacques J, Murdoch G, Whetsell W Jr, Kaye J, Manczak M. Differential loss of synaptic proteins in Alzheimer's disease: Implications for synaptic dysfunction. J Alzheimers Dis. 2005; 7:103–117. discussion 173–180. [PubMed: 15851848]
63. Nunomura A, Perry G, Aliev G, Hirai K, Takeda A, Balraj EK, Jones PK, Ghanbari H, Wataya T, Shimohama S, Chiba S, Atwood CS, Petersen RB, Smith MA. Oxidative damage is the earliest event in Alzheimer disease. J Neuropathol Exp Neurol. 2001; 60:759–767. [PubMed: 11487050]
64. Billings LM, Oddo S, Green KN, McGaugh JL, LaFerla FM. Intraneuronal Abeta causes the onset of early Alzheimer's disease-related cognitive deficits in transgenic mice. Neuron. 2005; 45:675–688. [PubMed: 15748844]
65. Leissring MA, Farris W, Wu X, Christodoulou DC, Haigis MC, Guarente L, Selkoe DJ. Alternative translation initiation generates a novel isoform of insulin-degrading enzyme targeted to mitochondria. Biochem J. 2004; 383:439–446. [PubMed: 15285718]
66. Schildgen V, Wulfert M, Gattermann N. Impaired mitochondrial gene transcription in myelodysplastic syndromes and acute myeloid leukemia with myelodysplasia-related changes. Exp Hematol. 2011; 39:666–675. e661. [PubMed: 21447369]
67. Arthur CR, Morton SL, Dunham LD, Keeney PM, Bennett JP Jr. Parkinson's disease brain mitochondria have impaired respirasome assembly, age-related increases in distribution of oxidative damage to mtDNA and no differences in heteroplasmic mtDNA mutation abundance. Mol Neurodegener. 2009; 4:37. [PubMed: 19775436]

Author Manuscript Author Manuscript Author Manuscript Author Manuscript

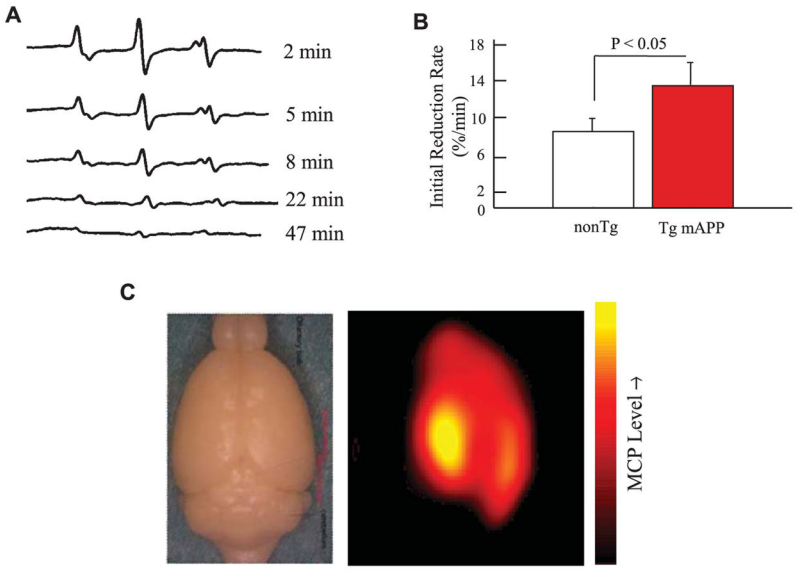

Fig. 1.

In vivo measurement and imaging of oxidative stress in the brain of mice. A) Time-course of EPR spectra of MCP in the brain *in vivo*. This panel shows representative EPR spectra acquired from a transgenic (Tg mAPP) mouse as a function of time after infusion of the redox probe. The spectrum is characteristic of MCP where the three peaks are due to hyperfine splitting from ^{14}N atom of the probe molecule. The spectra show the progressive decay of the probe, as the EPR-active nitroxide is bioreduced to EPR-silent hydroxylamine. Measurements were performed *in vivo* after infusion of the redox spin probe into carotid artery of an anesthetized mouse. B) Reduction rate of MCP in the brain *in vivo*. Initial reduction rate of the MCP redox probe during period of 2 to 7 min after infusion in the brain of Tg mAPP and nonTg mice (n = 4–5 per group) was used. The plot shows that the rate of bioreduction in Tg mAPP mice was significantly higher than that in nonTg mice, indicating that the brain of Tg mAPP mice had higher oxidative stress as compared to the nonTg mice. C) *In vivo* EPR imaging showing the localization of MCP in the brain. Typical distribution of the spin probe in the brain as measured at 30 min post-infusion. The spin probe was administered through carotid artery at a dose of 1 μL/g bw at 200 mM concentration.

Author Manuscript Author Manuscript Author Manuscript Author Manuscript

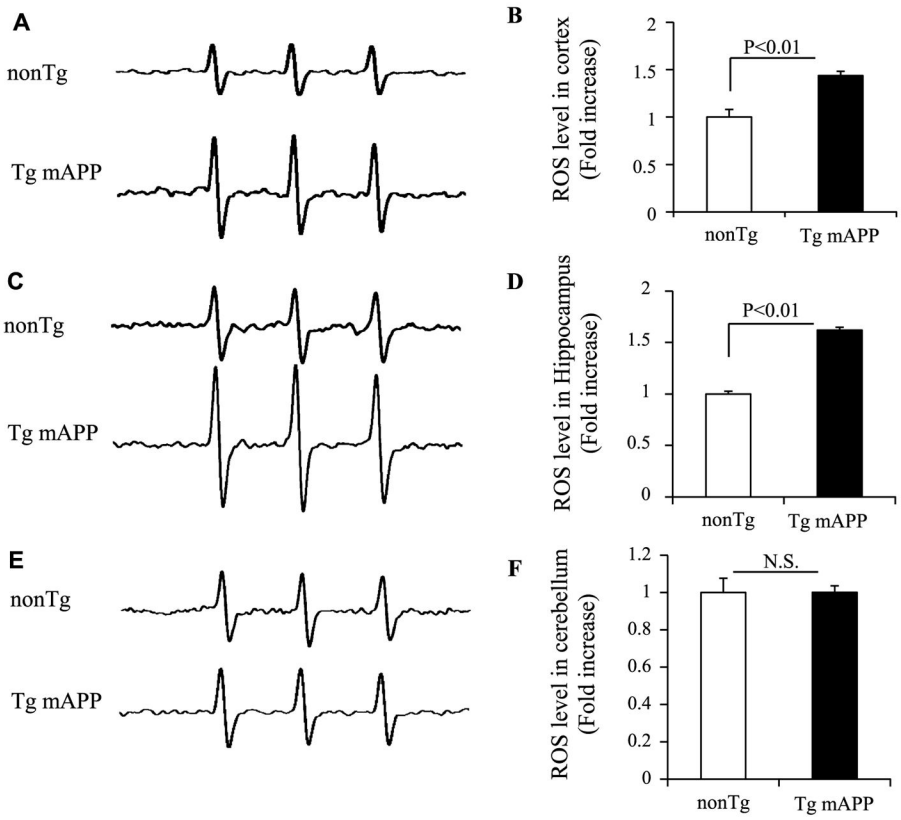

Fig. 2.

In vitro measurement of oxidative stress in the brain of mice at age of 8–9 month. Representative *in vitro* EPR spectra measured in the brain homogenates of cortex (A, B), hippocampus (C, D), and cerebellum (E, F) are shown. The peak height in the spectrum indicates levels of ROS. Quantification of EPR spectra in the indicated Tg mice (B, D, and F). $^{\#}p < 0.01$ compared to other groups of mice. Data are expressed as fold-increase relative to nonTg mice. $N = 3–4$ mice per group.

Author Manuscript Author Manuscript Author Manuscript Author Manuscript

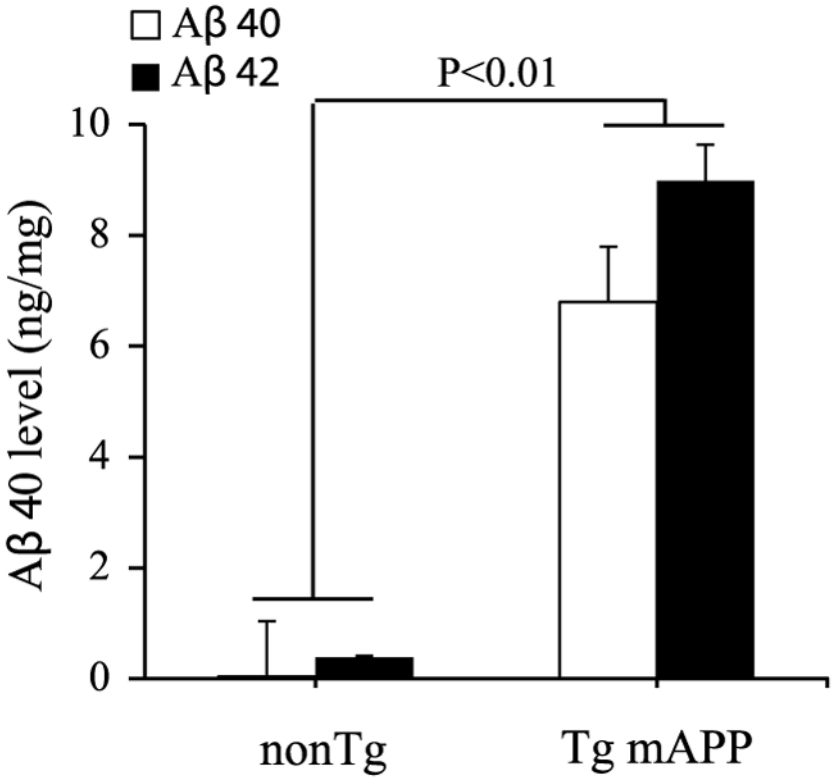

Fig. 3.

Increased Aβ levels in cerebral cortex of 8-month-old mAPP mice. Aβ levels in cerebral cortex from the indicated Tg mice were measured by ELISA. *N* = 3–4 mice per group.

Author Manuscript Author Manuscript Author Manuscript Author Manuscript

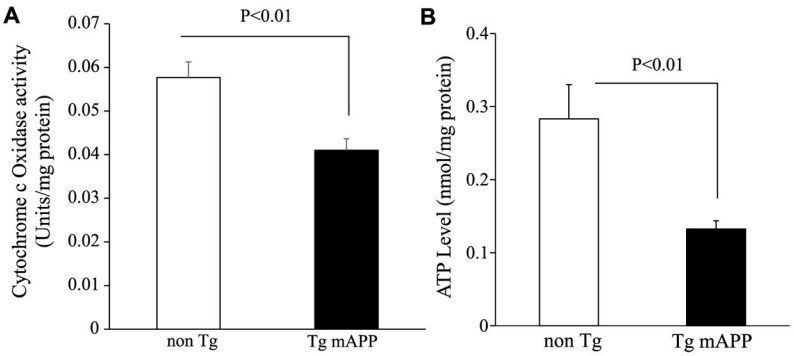

Fig. 4.

Cytochrome c oxidase activity in the cortex of mAPP mice and nonTg mice at 8–9 months of age. ATP levels in the cortex of 8–9-month old mAPP mice and nonTg mice. $N = 10$ mice per group.

Author Manuscript Author Manuscript Author Manuscript Author Manuscript

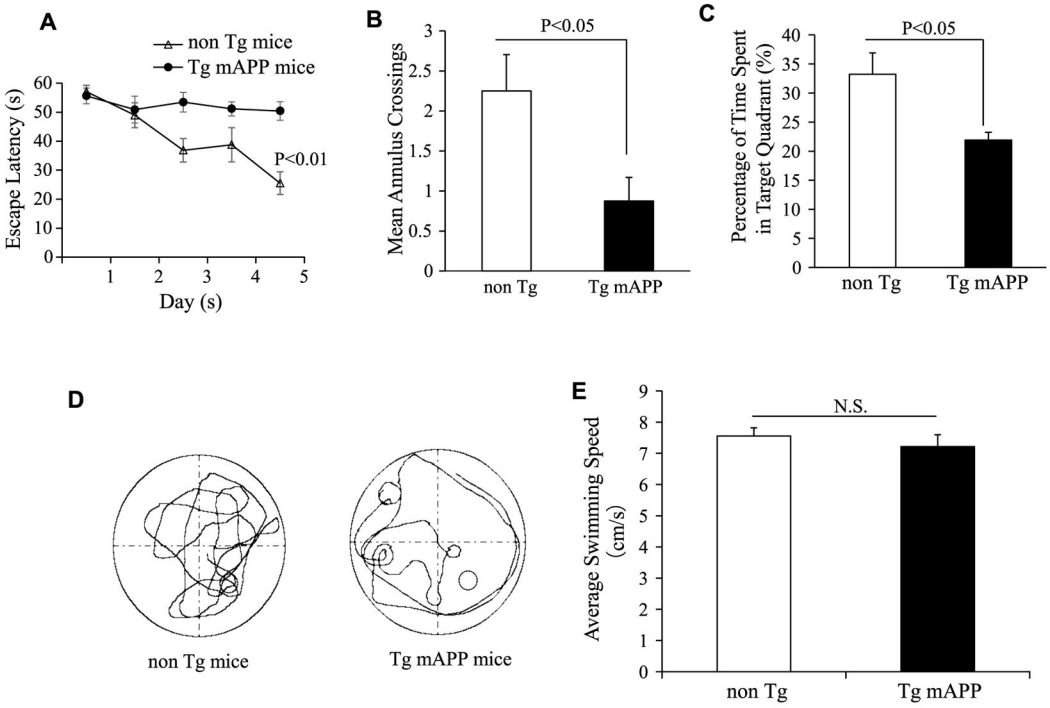

Fig. 5.

Spatial learning and memory of transgenic mAPP and nonTg mice at 8 months of age ($N = 8$ per group). Radial water maze test showed the average latency to escape to locate the hidden platform during each day of training sessions (A). $^{*}p < 0.01$ versus nonTg mice. The mean number of mice crossing the target quadrant during probe trials (B), and time spent in the target quadrant where the hidden platform is located (C). Pattern of representative searching traces for the indicated Tg mice in search of the target also indicated nonTg mice had better spatial learning and memory compared to mAPP mice (D). The transgenic mAPP mice and nonTg mice had similar swimming speed by the visual swimming speed test (E).